KA–TP–41–2013
LU TP 13–44
PSI–PR–13–17
WUB/13-19

Recommendations for the evaluation of Higgs production cross sections and branching ratios at the LHC in the Two-Higgs-Doublet Model

R. Harlander[1], M. Mühlleitner[2], J. Rathsman[3], M. Spira[4], O. Stål[5]

[1] *Fachbereich C, Bergische Universität Wuppertal, 42097 Wuppertal, Germany*

[2] *Institut für Theoretische Physik, Karlsruher Institut für Technologie KIT, 76131 Karlsruhe, Germany*

[3] *Department of Astronomy and Theoretical Physics Lund University, SE-223 62, Lund, Sweden*

[4] *Paul Scherrer Institut, CH–5232 Villigen PSI, Switzerland*

[5] *The Oskar Klein Centre, Department of Physics Stockholm University, SE-106 91 Stockholm, Sweden*

December 20, 2013

Abstract

In this note we give recommendations on how to evaluate LHC cross sections for (neutral) Higgs production and Higgs branching ratios in the general (CP-conserving) Two-Higgs-Doublet Model (2HDM). The current status of available higher-order corrections to Higgs production and decay in this model is discussed, and the existing public codes implementing these calculations are described. Numerical results are presented for a set of reference scenarios, demonstrating the very good agreement between the results obtained using different programs.

1 Introduction

The Two-Higgs-Doublet Model (2HDM) is one of the simplest extensions of the Standard Model (SM) Higgs sector. It can be useful both as a theoretical tool to explore the phenomenology of an extended Higgs sector, and to interpret experimental results from searches for additional Higgs bosons. A comprehensive review of this model is given in Ref. [1]. The existence of a Higgs boson with mass around $M_H = 125\,\text{GeV}$ and couplings compatible with the SM predictions already leads to severe restrictions of the 2HDM parameter space.

Precise analyses of the experimental data on the basis of the 2HDM require solid predictions of the relevant observables in this model. Two of the most important ones are the production cross sections and the branching ratios of the Higgs bosons. In this note, we provide a brief overview of the theory status of these quantities. We describe the available radiative corrections, and the most convenient tools that allow one to obtain numerical predictions for specific sets of 2HDM parameters. We also comment on current theoretical short-comings and open issues.

2 Theory recommendations

2.1 Cross sections

2.1.1 Higgs production in the Standard Model

The dominant production cross section for Higgs bosons in the Standard Model is gluon fusion. The coupling of the gluons to the Higgs boson is mediated predominantly by a top quark loop, while loops from other quarks are suppressed by their Yukawa couplings. The effect of bottom quark loops amounts to about -6%, charm quark loops reach about -1%. QCD corrections to the gluon fusion cross section are large, reaching more than a factor of two at NNLO QCD [2–4]. While the NLO QCD corrections can be calculated for general quark mass [5–7], the NNLO terms are available only in the heavy-top approximation. The validity of this approximation has been checked to be better than 1% for Higgs masses below 300 GeV [8–12].

Various effects beyond fixed order perturbative corrections have been studied, but they are not included in `SusHi` [13] or `HIGLU` [14] (see below). They include soft gluon resummation [15, 16] (which, as has been argued, can be accounted for by choosing the renormalization/factorization scale to $\mu = M_H/2$ [17]), and partial or approximate N^3LO results [16, 18, 19].

Electroweak corrections are also known [20–23], and a calculation of the mixed electroweak/QCD effects [17] – albeit in the unphysical limit $M_W > M_H$ – suggests that they approximately factorize from the QCD effects, since the latter are dominated by soft-gluon radiation.

2.1.2 Higgs production in the 2HDM

The calculation of the gluon fusion cross section for scalar Higgs bosons in the 2HDM differs from the SM only by the Higgs couplings. Therefore the QCD corrections in the 2HDM can be obtained quite trivially by separately rescaling the SM expressions for the top- and bottom-loop induced amplitudes. Note, however, that the bottom-loop contribution can be enhanced in the 2HDM. Since NNLO corrections are only known for the top-loop contribution, the accuracy of the prediction decreases with increasing values of the ratio g_b/g_t, where g_q is the $Hq\bar{q}$ coupling. An analogous procedure can be applied for the pseudoscalar Higgs boson if the individual scalar amplitudes are replaced by the corresponding pseudoscalar ones.

Note also that electroweak effects are only fully available in the SM. However, the electroweak corrections involving light quarks (i.e. all but the top quark) are known separately [23]; since they are proportional to the VVH coupling, where $V \in \{W, Z\}$, they can also be rescaled quite easily from the SM to the 2HDM. They do not contribute to pseudoscalar Higgs boson production, since the pseudoscalar does not couple to W, Z bosons at tree level.

If the ratio g_b/g_t is sizable, another production mechanism comes into play, namely associated $\phi b\bar{b}$ ($\phi = h, H, A$) production [24–29]. Its fully inclusive cross section can be calculated through NNLO in the 5-flavor scheme (5FS) [30], which effectively corresponds to the process $b\bar{b} \to \phi$. The corresponding 4-flavor-scheme (4FS) numbers can be generated by using the grids for the corresponding MSSM cross sections [31] and inserting the appropriate factors for the bottom Yukawa couplings. Both calculations can finally be merged by using the Santander matching [32].

2.1.3 The invalidity of global K-factors

As described in Section 2.1.2, the result for the gluon fusion cross section $gg \to \phi$, where ϕ represents both the light h and the heavy H CP-even Higgs boson of the 2HDM, can be obtained by replacing the Yukawa couplings in the SM amplitude by their 2HDM values. One may wonder whether it is sufficient for the inclusive Higgs boson production cross section to apply this rescaling only at LO and take the QCD corrections into account as

an overall factor [33]:

$$\sigma_{\text{2HDM}}^{\text{approx}} \stackrel{?}{=} \frac{\sigma_{\text{SM}}^{\text{NNLO}}}{\sigma_{\text{SM}}^{\text{LO}}} \left\{ g_t^2 \sigma_{tt}^{\text{LO}} + g_t g_b \sigma_{tb}^{\text{LO}} + g_b^2 \sigma_{bb}^{\text{LO}} \right\} , \tag{1}$$

where $\sigma_{\text{SM}}^{\text{LO}} = \sigma_{tt}^{\text{LO}} + \sigma_{tb}^{\text{LO}} + \sigma_{bb}^{\text{LO}}$, with σ_{tt} and σ_{bb} the contributions due to the top and the bottom loop, respectively, and σ_{tb} arising from the top-bottom interference. The coefficients $g_{t,b}$ denote the top and bottom Yukawa couplings, normalized to the SM ones. They depend only on the Higgs mixing angles α and β in general. This approach assumes that the relative QCD corrections are about the same for all three parts. This hypothesis, however, can be checked explicitly by comparing the individual numbers at LO, NLO and NNLO. In Table 1 the results (obtained with `HIGLU` [14] and cross-checked with `SusHi` [13]) are displayed for the LHC at 8 TeV c.m. energy and in Table 2 for 14 TeV. While the pure top-loop contributions exhibit the known large K-factors, this is not the case for the tb-interference nor for the pure bottom loops. The approximation of Eq. (1) is therefore off by up to 50% for cases in which the bottom loops provide the dominant contributions. Note in particular that the QCD corrections to the interference term σ_{tb} are always moderate and can be of either sign. Assuming a "global K-factor" is therefore clearly invalid; instead, the full NLO (NNLO) calculation has to be used in order to obtain reliable results beyond LO. Fortunately, they can easily be obtained with the help of `SusHi` [13] or `HIGLU` [14].

2.2 Transverse momentum distribution

Just like the inclusive cross section, the transverse-momentum (p_T) distribution of the SM Higgs boson in gluon fusion is predominantly mediated by top-quark loops, giving rise to the process $gg \to gH$, supplemented by the subleading channels $gq \to qH$ and $q\bar{q} \to gH$ [34], see Fig. 1. However, since the bottom quark contribution amounts to about -6% in the inclusive cross section, we also expect a similar effect on the p_T-distribution. At leading order, the bottom quark contribution is only sizable for small p_T, while for larger p_T values it can safely be neglected. The NLO corrections to the p_T-distribution are only known in the heavy-top limit [35][1], including subleading terms in the inverse top mass at NLO [37]. Similar to the inclusive cross section, the QCD corrections are large, nearly doubling the rate at finite p_T values.

It is well-known that the pure LO and NLO results diverge towards $p_T \to 0$. The small p_T region thus requires a soft gluon resummation in order to achieve a reliable prediction. This resummation has been performed systematically for the top quark loops in Ref. [38], neglecting finite top mass effects at NLO. Since soft gluon effects factorize, the top mass effects at small p_T are well approximated by the LO mass dependence for small Higgs

[1] In this approximation, the gg-component for this process was even calculated at NNLO [36].

M_H [GeV]	σ_{tt} [pb]	σ_{tb} [pb]	σ_{bb} [pb]	σ_{tot} [pb]
	(LO)	(LO)	(LO)	(LO)
125.0	10.32	-1.241	0.1131	9.188
125.5	10.23	-1.225	0.1108	9.116
126.0	10.15	-1.210	0.1085	9.044
150.0	7.012	-0.6770	0.04330	6.379
200.0	3.788	-0.2465	0.009013	3.551
250.0	2.395	-0.1093	0.002540	2.288
300.0	1.748	-0.05662	0.0008719	1.692
	(NLO)	(NLO)	(NLO)	(NLO)
125.0	17.32	-1.206	0.1357	16.25
125.5	17.18	-1.192	0.1330	16.12
126.0	17.04	-1.178	0.1303	15.99
150.0	11.90	-0.6920	0.05293	11.26
200.0	6.518	-0.2694	0.01133	6.260
250.0	4.159	-0.1250	0.003257	4.037
300.0	3.061	-0.06705	0.001135	2.995
	(NNLO)	(NLO)	(NLO)	(mixed)
125.0	20.18	-1.206	0.1357	19.11
125.5	20.02	-1.192	0.1330	18.96
126.0	19.85	-1.178	0.1303	18.81
150.0	13.78	-0.6920	0.05293	13.14
200.0	7.490	-0.2694	0.01133	7.231
250.0	4.754	-0.1250	0.003257	4.633
300.0	3.485	-0.06705	0.001135	3.419

Table 1: *SM Higgs production cross sections via gluon fusion at leading order (LO), next-to-leading order (NLO) and including the next-to-next-to-leading order (NNLO) corrections to the top loops in the heavy-top limit on top of the next-to-leading order predictions using MSTW2008 PDFs for* $\sqrt{s} = 8$ *TeV. The renormalization and factorization scales have been chosen as* $\mu_R = \mu_F = M_H/2$.

M_H [GeV]	σ_{tt} [pb]	σ_{tb} [pb]	σ_{bb} [pb]	σ_{tot} [pb]
	(LO)	(LO)	(LO)	(LO)
125.0	27.92	-3.360	0.3061	24.87
125.5	27.72	-3.320	0.3001	24.70
126.0	27.51	-3.281	0.2942	24.52
150.0	19.85	-1.916	0.1226	18.05
200.0	11.60	-0.7547	0.02760	10.87
250.0	7.860	-0.3588	0.008335	7.509
300.0	6.112	-0.1980	0.003048	5.917
	(NLO)	(NLO)	(NLO)	(NLO)
125.0	44.05	-2.799	0.3302	41.58
125.5	43.74	-2.770	0.3239	41.29
126.0	43.43	-2.741	0.3177	41.01
150.0	31.72	-1.695	0.1351	30.16
200.0	18.88	-0.7236	0.03144	18.19
250.0	12.96	-0.3634	0.009741	12.60
300.0	10.18	-0.2094	0.003635	9.979
	(NNLO)	(NLO)	(NLO)	(mixed)
125.0	51.61	-2.799	0.3302	49.14
125.5	51.24	-2.770	0.3239	48.79
126.0	50.87	-2.741	0.3177	48.44
150.0	36.91	-1.695	0.1351	35.35
200.0	21.77	-0.7236	0.03144	21.08
250.0	14.85	-0.3634	0.009741	14.50
300.0	11.62	-0.2094	0.003635	11.42

Table 2: *Same as Table 1, but for* $\sqrt{s} = 14$ *TeV.*

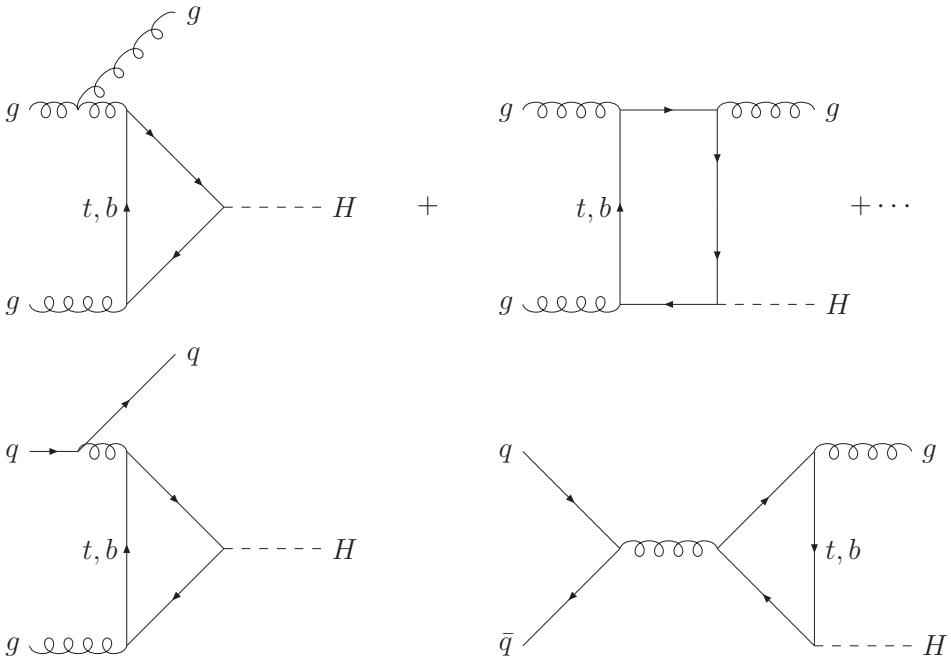

Figure 1: *Typical Feynman diagrams contributing to Higgs + jet production emerging from gg, qg and $q\bar{q}$ initial states.*

masses [39–41]. As long as the top-loop contribution dominates the cross section, the only limiting factor of the NLO+NNLL result as implemented in `HqT` or `HRes` [42] is thus the heavy-top approximation of the NLO corrections which affects the small p_T range for large Higgs masses and the large p_T region.

Recently, bottom quark contributions have been included in the predictions for the resummed p_T-distributions [39–41, 43, 44]. It was shown [43, 44] that factorization of the soft gluon effects fails in this case if the resummation scale is chosen to be of the order of the Higgs mass, as it is done for the top-loop contributions.

In Ref. [43], it was therefore suggested to introduce an additional resummation scale of the order of m_b for the terms involving bottom quark loops. Due to the relatively large separation of scales (m_b, M_H, p_T), certain potentially large logarithms remain, which are still treated perturbatively in this approach. The relative theoretical uncertainty is thus much larger than for the top quark terms. This adds to the fact that the bottom

loop contributions can only be included at LO+LL, since the QCD corrections to the p_T-distribution are unknown. Due to the small bottom Yukawa coupling, the impact on the overall theoretical uncertainty is rather modest in the SM though.

This is in contrast to 2HDM scenarios with a largely enhanced bottom Yukawa coupling. The resulting theoretical uncertainty of the differential cross section $d\sigma/dp_T$ could be of the order of 100% in the whole p_T region. Analogously large uncertainties also arise for the shape of the p_T distribution, i.e. the normalized differential cross section $1/\sigma\ d\sigma/dp_T$, since unresummed large logarithms at small p_T typically have an impact on the high-p_T region due to the unitarity constraint given by the total cross section. For the time being, we recommend the use of the implementation of mass effects in the `POWHEG box` [40] and `MC@NLO` [45, 46] for the Higgs p_T distributions, since both codes include LO quark mass effects consistently.

Let us now turn to the transverse momentum distribution in associated production of a Higgs boson with bottom quarks. Similar to the inclusive cross section, the p_T distribution of the Higgs bosons can also be obtained both in the 4FS and the 5FS [47]. In the 5FS, the NLO prediction (i.e., without resummation) has been calculated in Ref. [48]. Note that in the 5FS the Higgs can be produced at finite p_T only when a jet is emitted from the initial state, similar to the situation in gluon fusion. Imposing the restriction that this jet be due to a b-quark, the NLO result was found in Ref. [25, 48] and is implemented in `MCFM` [49]. Also the case with two final state b quarks was considered there, albeit only at LO in the 5FS. The effect of a p_T-, jet-, or b-jet-veto through NNLO was considered in Ref. [50]; a fully differential Monte Carlo program for $b\bar{b}H$ production in the 5FS was presented in Ref. [51]. None of these results are applicable for small p_T where logarithms spoil the perturbative convergence. The LO+LL resummation of these terms, on the other hand, can be found in Ref. [52].

In the 4FS calculation, the Higgs boson can be produced at finite p_T already at LO. One could attempt to match the NLO 4FS [28, 29] with the 5FS results [25, 48] along the lines of Ref. [32] in order to obtain the most accurate prediction of the Higgs p_T distribution. This holds independent of the number of b-tags in the final state: for zero and one b-tag, both 4FS and 5FS results are formally of NLO, for two b-tags, the 5FS result is available only at LO, while the 4FS result is still valid through NLO. Note, however, that even in the latter case, both approaches include partly complementary terms because the arrangement of the perturbative series is different in the 4FS and the 5FS.

Unfortunately, we are not aware of any attempts to match 4FS and 5FS results for the Higgs p_T distribution in associated $b\bar{b}H$ production. Even public tools for the calculation of the general NLO or resummed Higgs p_T distribution in either of the two schemes are unavailable to our knowledge. Given sufficient demand from the experimental community, we would expect this to change quite quickly though. Until then, we recommend to

contact the authors of the papers referred to in this section in order to obtain predictions for particular sets of parameters, or to resort to tools like `MCFM` [49] or `aMC@NLO` [53], for specific purposes.

2.3 Branching ratios

The decay widths and branching ratios of the 2HDM Higgs bosons are usually calculated at leading order in the 2HDM parameters. This is the case for both public codes, `2HDMC` [54] and `HDECAY` [55, 56], which are available to calculate the 2HDM decays. Using tree-level relations to convert between different parametrizations (e.g. physical masses and quartic couplings), the results obtained with input in different bases are formally equivalent. However, unlike the case of the SM with $M_H = 125$ GeV or the MSSM, there is no automatic protection in the 2HDM against arbitrarily large quartic couplings, which may lead to a violation of perturbativity of the couplings and tree-level unitarity. This should be kept in mind when calculating decay widths involving triple-Higgs couplings, such as $h \to \gamma\gamma$ or $H \to hh$. To ensure reasonable theoretical properties of the model, we recommend that positivity of the Higgs potential, perturbativity of the couplings and tree-level unitarity is applied as explicit constraints on the 2HDM scenarios in all analyses.

Higher-order SM electroweak corrections do not factorize from the LO result and cannot be readily included for the 2HDM. There is currently no calculation of the electroweak corrections to the 2HDM Higgs decays available in usable format. We therefore recommend that electroweak corrections are not included in the calculation of 2HDM branching ratios, and in particular that no corrections obtained for the SM are applied. This introduces unavoidable uncertainties, which can be estimated from the size of the known electroweak corrections within the SM to be up to 5–10% for several partial decay widths. Differences of this magnitude compared to the most precise values for the SM are therefore expected even in the decoupling limit.

A consistent comparison of 2HDM predictions in the decoupling limit to SM values furthermore requires that the limit is taken properly so that no residual 2HDM effects are present, e.g. from $H^\pm$ loop contributions to $h \to \gamma\gamma/Z\gamma$. Using the physical Higgs mass basis as an example (see below), SM-like decays for the lightest 2HDM Higgs boson can be achieved by choosing $M_h \sim 125$ GeV, $\sin(\beta - \alpha) = 1$, $M_H, M_A, M_{H^\pm} \gg v$, and the value of M_{12}^2 which makes the hH^+H^- coupling vanish.

Unlike the electroweak corrections, many of the QCD corrections (which typically are numerically significant) *do* factorize, and can therefore be taken over directly from the corresponding SM or MSSM calculations. For numerically relevant branching ratios, we recommend that QCD corrections are taken into account to the highest degree of accuracy that is practically possible.

Schematically, the widths for the SM-type decays to quark pairs and vector bosons are obtained at leading order from their SM equivalents by rescaling the interaction vertices with the corresponding 2HDM factors. The loop-mediated decay to gluons also proceeds as in the SM, with the appropriate rescaling of the Yukawa couplings. For the remaining decays it is necessary in addition to take 2HDM-specific contributions into account. Even with the restriction to models which respect perturbativity of the couplings and tree-level unitarity, it is not possible to à-priori assume that any of these contributions are small over the 2HDM parameter space. This is true in particular for the decays to vector bosons and Higgs bosons, $\phi_i \to \phi_j V$ ($V = W/Z$), or Higgs-to-Higgs-Higgs decays, $\phi_i \to \phi_j \phi_k$, which can both be important when kinematically allowed. The resulting decay patterns could therefore differ substantially from that of a SM-like Higgs boson with the same mass.

We recommend that a full 2HDM calculation of the branching ratios is always performed for each parameter point under study, as can easily be obtained using either `2HDMC` [54] or `HDECAY` [55, 56]. This is important to get both the individual contributions (including higher-order corrections) and the total width (and, therefore, the branching ratios) correct. It is *not* recommended to rely on any simplified approximations in this respect.

3 Available programs

3.1 Comparison of `HIGLU` and `SusHi`

The order of the QCD corrections to the gluon fusion cross section implemented in `SusHi` [13] and `HIGLU` [14] is identical, although they are evaluated in completely independent and partly quite different ways. They include the full NLO QCD corrections, taking into account all quark mass effects, for the top-, bottom- and charm-loop contributions. NNLO QCD corrections are included only for the top quark by applying the heavy-top limit. Both `SusHi` and `HIGLU` allow one to modify the top and bottom Yukawa couplings through the input file. For the SM, both programs also apply the electroweak correction factor, assuming full factorization of the QCD effects.

`SusHi` also evaluates the cross section for $b\bar{b} \to \phi$ ($\phi \in \{h, H, A\}$) through NNLO QCD within the 5-flavor scheme. It also provides a link to `2HDMC` which allows for a number of different parametrizations of the 2HDM, immediately passes on the correct values of the Higgs couplings to `SusHi`, and evaluates the Higgs decay rates. `SusHi` takes into account electroweak corrections to the 2HDM cross section as induced by light-fermion loops, see Section 2.1.2.

`HIGLU` is linked to `HDECAY` thus allowing for a consistent use together with the 2HDM extension of `HDECAY`.

3.2 Comparison of 2HDMC and HDECAY

The C++ code 2HDMC

2HDMC [54] is a public C++ code available for download from HepForge through `http://2hdmc.hepforge.org/`. It has been developed from the start as a tool for studies in the (CP-conserving) two-Higgs-doublet model. As such, it contains an implementation of the general form for the 2HDM potential [57]. There are a number of different options available to specify the model parameters, which include:

Generic basis

Quartic potential couplings:	$\lambda_1, \lambda_2, \lambda_3, \lambda_4, \lambda_5, \lambda_6, \lambda_7$
Soft Z_2-breaking mass:	M_{12}^2 (GeV^2)
Ratio of vacuum expectation values (basis):	$\tan\beta$

Physical basis

Higgs boson masses:	$M_h, M_H, M_A, M_{H^\pm}$ (GeV)
Basis invariant scalar mixing:	$\sin(\beta-\alpha)$
Z_2-breaking quartic couplings:	λ_6, λ_7
Soft Z_2-breaking mass:	M_{12}^2 (GeV^2)
Ratio of vacuum expectation values (basis):	$\tan\beta$

For details on the definitions of these input parameters, see [54]. Note that 2HDMC uses the convention $-\frac{\pi}{2} \leq \beta - \alpha \leq \frac{\pi}{2}$, and that the *physical* basis (with $\lambda_6 = \lambda_7 = 0$) is equivalent to the input used by HDECAY (see below). A model specified using one input can be translated between different parameter bases by 2HDMC.

Independent of the choice of model parametrization, 2HDMC allows the 2HDM Yukawa sector to be specified in the most general way as full (3×3) Yukawa matrices using the language of [57]. The case of (softly-broken) Z_2-symmetric 2HDM *types* I–IV, as defined in [58], is also available. These recommendations concern only this class of models.

2HDMC contains functions to test for consistency of the specified model parameters, such as vacuum stability (at the input scale), tree-level unitarity, and perturbativity of the couplings. It can also evaluate one-loop contributions to the oblique electroweak parameters and direct experimental constraints through an interface to the code HiggsBounds [59]. The Higgs decay modes are calculated in 2HDMC using the full 2HDM parametrization and a general Yukawa sector, including tree-level FCNCs in models where they are present.

The Fortran code HDECAY

The Fortran code HDECAY [55, 56] has been extended to include the computation of the Higgs boson decay widths in the framework of the 2HDM. The input parameters to be

specified in the input file `hdecay.in` are

the mixing angle:	α
the ratio of the vacuum expectation values:	$\tan\beta$
the mass values of the five Higgs bosons:	$M_h, M_H, M_A, M_{H^\pm}$ (GeV)
the mass parameter squared:	M_{12}^2 (GeV^2)

and a flag specifying the type of the 2HDM. The models type I–IV are implemented. From the input parameters `HDECAY` calculates the couplings which are needed in the computation of the decay widths. With the appropriate coupling replacements according to the various 2HDM's, the decay widths are the same as for the MSSM Higgs boson decays, which are already included in the program. Only the SUSY particle contributions in the loop-mediated decays and the decays into SUSY particles as well as higher order corrections due to SUSY particle loops have been turned off for the 2HDM case.

Decay modes

The implemented decay widths and higher order corrections are specified in the following for both codes, `2HDMC` (version 1.6.2) and `HDECAY` (version 6.00).

Decays into quark pairs: The QCD corrections factorize with respect to the tree-level amplitude and can therefore be taken over from the SM case. For the neutral Higgs decays the fully massive NLO corrections near threshold [60] and the massless $\mathcal{O}(\alpha_s^4)$ corrections far above threshold [61–63] have been included in `HDECAY`. They are calculated in terms of the running quark masses and of the running strong coupling constant in order to resum large logarithms. The QCD corrections to the charged Higgs boson decays have been taken from [64]. Note that for the higher order corrections to the decay widths only QCD corrections are taken into account, as the electroweak corrections cannot be adapted from the SM case. For the decays of the heavier neutral Higgs bosons into a top quark pair, in `HDECAY` off-shell decays below threshold have been implemented as well as for the decays of a charged Higgs boson into a top-bottom quark pair [65].

In `2HDMC` all decays into on-shell light quark pairs are included. Far above the threshold, the dominant QCD corrections for the decays to pairs of strange, charm, and bottom quarks are taken into account by absorbing large logarithms into the running quark masses appearing in the Yukawa couplings at a scale set by the decaying Higgs boson mass [60]. QCD corrections in this limit are included to NNLO, $\mathcal{O}(\alpha_s^2)$ [61], for the neutral Higgs decays. For the decay to $t\bar{t}$, in `2HDMC` threshold corrections of $\mathcal{O}(\alpha_s)$ are calculated according to [60], keeping the full dependence on m_t. Below threshold, the contributions from the off-shell decay $h/H/A \to t\bar{t}^{(*)} \to t\bar{b}W^- +$ c.c. are included according to [65]. The calculations of charged Higgs decays in `2HDMC` contain the $\mathcal{O}(\alpha_s)$ QCD corrections from [64], with full mass dependence near threshold for $H^+ \to tb$. Below threshold, the three-body decay $H^+ \to t^{(*)}\bar{b} \to \bar{b}bW^+ +$ c.c. is included according to [65].

Decays into gluons: The QCD corrections to the neutral Higgs boson decays into gluons, a loop-induced process already at leading order, can be taken over from the SM, respectively, the MSSM. They have been included up to N^{3}LO in `HDECAY`. While for the SM at NLO the full quark mass dependence [7] is available, for the 2HDM the corrections have been taken into account in the limit of heavy-quark loop particle masses [66–68].

As in `HDECAY` the contributions from all colored fermions are included to one loop in `2HDMC`. For the contribution from the top quark loop, $\mathcal{O}(\alpha_s^2)$ NNLO QCD corrections are included in the heavy-top limit [67].

Decays into photon pairs: The decay to a photon pair is loop-mediated, with the two most important SM contributions being due to the top quark and W boson loops. In the 2HDM, there is also a H^+ contribution which becomes numerically significant in some cases. The bottom loop becomes relevant for the photonic decay rate in scenarios with enhanced bottom Yukawa couplings. For this decay, a special running quark mass is employed to capture QCD corrections [69] in `2HDMC` (the same as used in `HDECAY`). Explicit corrections to the top quark contribution in the heavy-top limit (neglecting the mass dependence) are included to $\mathcal{O}(\alpha_s)$ [70]. In the pseudoscalar case only heavy charged fermion loops contribute.

In `HDECAY` the neutral Higgs boson decays into a photon pair have been implemented at NLO QCD including the full mass dependence for the quarks [7, 69, 71].

Decays into $Z\gamma$: The loop induced decays of scalar Higgs bosons into $Z\gamma$ are mediated by W and heavy charged fermion loops, while the pseudoscalar decays proceed only through charged fermion loops. The QCD corrections to the quark loops are numerically small [72] and have not been taken into account in `2HDMC` nor in `HDECAY`.

Decays into massive gauge bosons: The decay widths of the scalar Higgs bosons into massive gauge bosons $\phi \to V^{(*)}V^{(*)}$ ($V = W, Z$) are the same as the SM decay width after replacing the SM Higgs coupling to gauge bosons with the corresponding 2HDM Higgs coupling. The option of double off-shell decays [73] has been included in `2HDMC` and `HDECAY`. The pseudoscalar Higgs boson does not decay into massive gauge bosons at tree level.

Decays into Higgs boson pairs: The heavier Higgs particles can decay into a pair of lighter Higgs bosons. This is a feature of the 2HDM which does not exist in the SM. Due to more freedom in the mass hierarchies compared to the MSSM case, the following Higgs-to-Higgs decays are possible and have been included in `2HDMC` and `HDECAY`,

$$h \to AA^{(*)}\,, \qquad H \to hh^{(*)}\,, \qquad H \to AA^{(*)}\,. \tag{2}$$

In addition the decays into a charged Higgs boson pair are possible,

$$h \to H^+H^-\,, \qquad H \to H^+H^-\,. \tag{3}$$

In both programs all decays are calculated at leading order, retaining the full parameter dependence of the 2HDM for the trilinear couplings. The contributions from final states with an off-shell scalar or pseudoscalar, which can be significant, have been taken into account in HDECAY [65]. It is important to note that the partial width for these decays can grow very large for parameter points that do not respect the requirements of perturbativity and tree-level unitarity.

Decays into a gauge and Higgs boson pair: The Higgs boson decays into a gauge and a Higgs boson [56], which have been implemented in both programs, including the possibility of off-shell gauge bosons [65], are given by

$$\begin{array}{llllllllll} h & \to & AZ^{(*)}\,, & h & \to & H^\pm W^{\mp(*)}\,, & & & & \\ H & \to & AZ^{(*)}\,, & H & \to & H^\pm W^{\mp(*)}\,, & & & & \\ A & \to & hZ^{(*)}\,, & A & \to & HZ^{(*)}\,, & A & \to & H^\pm W^{\mp(*)}\,, \\ H^\pm & \to & hW^{\pm(*)}\,, & H^\pm & \to & HW^{\pm(*)}\,, & H^\pm & \to & AW^{\pm(*)}\,. \end{array} \tag{4}$$

They have been implemented at leading order and include the contributions of off-shell W and Z bosons below threshold [65].

4 Numerical results

The programs dicussed in these recommendations, SusHi, HIGLU, 2HDMC and HDECAY, all implement the most general (CP-conserving) version of the 2HDM with a softly-broken Z_2-symmetry, i.e. type I–IV models. In the following we define three reference scenarios of this type in order to compare and discuss differences between the codes for the evaluation of cross sections and decay rates. Please note that these scenarios have been chosen arbitrarily, and should not be interpreted as benchmark scenarios for 2HDM searches. The input parameters for these scenarios are given in Table 3. For the numerical results presented below we have adopted values for the SM parameters according to Appendix A. Of course, the quoted reference values for the 2HDM cross sections and branching ratios depend sensitively on these parameter settings.

4.1 Cross sections

Tables 4–6 show the cross sections for scenarios A, B, and C as evaluated with SusHi and HIGLU. The columns denoted "%" show the percental deviation between the SusHi and the HIGLU result, defined as

$$\Delta \equiv 2\left|\frac{\sigma_{\texttt{SusHi}} - \sigma_{\texttt{HIGLU}}}{\sigma_{\texttt{SusHi}} + \sigma_{\texttt{HIGLU}}}\right|\,. \tag{5}$$

Parameter	Scenario A	Scenario B	Scenario C
Common parameters			
Type	I	II	II
M_h (GeV)	125	125	125
M_H (GeV)	300	300	400
M_A (GeV)	330	270	500
$M_{H^\pm}$ (GeV)	230	335	550
M_{12}^2 (GeV^2)	25600	1798	15800
$\tan\beta$	1.5	50	10
2HDMC			
$\sin(\beta-\alpha)$	0.901314	0.999001	0.999
λ_6	0	0	0
λ_7	0	0	0
HDECAY			
α	-0.14	0.0247	-0.0549436

Table 3: Values of the input parameters for the 2HDM reference scenarios.

We have checked that the agreement between these two programs in all cases is better than 0.1% if the same set of corrections is taken into account. The numerical differences observed in the tables for the CP-even Higgs bosons are due to the electroweak corrections taken into account by SusHi, as described in Section 2.1.2. For the CP-odd Higgs boson, these corrections are absent due to the vanishing AVV coupling at tree level.

The numbers listed in the tables correspond to our recommendations for the central values of the cross section, which are obtained with the central MSTW2008 parton density sets. For gluon fusion, the renormalization and factorization scale is set to $\mu_F = \mu_R = M_\phi/2$, where $\phi \in \{h, H, A\}$. Theoretical uncertainties should be determined by varying μ_F and μ_R independently within a factor of two around $M_\phi/2$. For $b\bar{b}\phi$ production in the 5FS, we use $\mu_R = M_\phi$ and $\mu_F = M_\phi/4$ [27, 30] as central scales. The scale uncertainty can be obtained as suggested in Ref. [30, 74] by varying μ_F within the interval $[0.1, 0.7]M_\phi$ and μ_R within $[1/5, 5]M_\phi$. PDF uncertainties for the 5FS can be estimated following the recommendation of the PDF4LHC group [75]. In the 4FS numbers of Ref. [31], it is[2] $\mu_F = \mu_R = M_\phi/4$. The uncertainties have been obtained by varying both μ_F and μ_R within the interval $[M_\phi/8, M_\phi/2]$.

In addition, the uncertainty due to the undetermined renormalization scheme for the bottom Yukawa coupling should be taken into account. Clearly, its impact on the 2HDM cross section prediction can be much more severe than in the SM, in particular in type II

[2] In Ref. [74], it is stated by mistake that the Yukawa coupling is renormalized at $\mu_R = M_\phi$.

models with large $\tan\beta$. Consider, for example, the results for reference scenario B at 14 TeV. The total cross sections for the three Higgs bosons can be decomposed as

$$\begin{aligned}
\sigma(gg \to h) &= 55.55\ (0.93 + 0.06 + 0.01)\,\text{pb} + 2.23\,\text{pb}\,, \\
\sigma(gg \to H) &= 8.837\ (0.00 - 0.03 + 1.03)\,\text{pb} + 0.007\,\text{pb}\,, \\
\sigma(gg \to A) &= 16.49\ (0.00 - 0.03 + 1.03)\,\text{pb}\,,
\end{aligned} \tag{6}$$

where the first and the third number in brackets correspond to the pure top and bottom quark contribution, respectively, and the second number to the interference term. The last term, which is added to the total result, corresponds to the electroweak corrections. For the heavy Higgs bosons H, A the bottom loops provide by far the dominant contribution in scenario B. The associated uncertainties are sizable due to the choice of the bottom mass inside the loops and the bottom Yukawa coupling and should be taken over from the corresponding analyses within the MSSM working group, see [31].

$\sqrt{s}$	$\sigma(gg \to h)$/pb			$\sigma(gg \to H)$/pb			$\sigma(gg \to A)$/pb		
/TeV	SusHi	HIGLU	%	SusHi	HIGLU	%	SusHi	HIGLU	%
7	22.00	21.25	3.5	0.07199	0.06996	2.9	4.061	4.063	0.05
8	28.03	27.07	3.5	0.09897	0.09617	2.9	5.639	5.642	0.06
13	63.96	61.79	3.5	0.2846	0.2766	2.9	16.69	16.70	0.04
14	72.05	69.60	3.5	0.3305	0.3212	2.8	19.45	19.46	0.04

Table 4: Gluon fusion cross sections for scenario A.

$\sqrt{s}$	$\sigma(gg \to h)$/pb			$\sigma(gg \to H)$/pb			$\sigma(gg \to A)$/pb		
/TeV	SusHi	HIGLU	%	SusHi	HIGLU	%	SusHi	HIGLU	%
7	17.91	17.22	3.9	2.025	2.023	0.1	3.979	3.978	0.03
8	22.76	21.88	3.9	2.759	2.756	0.1	5.355	5.354	0.03
13	51.37	49.40	3.9	7.660	7.652	0.1	14.35	14.34	0.05
14	57.78	55.56	3.9	8.844	8.835	0.1	16.49	16.48	0.06

Table 5: Gluon fusion cross sections for scenario B.

$\sqrt{s}$	$\sigma(gg \to h)$/pb			$\sigma(gg \to H)$/pb			$\sigma(gg \to A)$/pb		
/TeV	SusHi	HIGLU	%	SusHi	HIGLU	%	SusHi	HIGLU	%
7	16.17	15.47	4.4	0.02707	0.02702	0.2	0.02421	0.02422	0.05
8	20.59	19.70	4.4	0.03821	0.03814	0.2	0.03575	0.03576	0.03
13	46.88	44.86	4.4	0.1179	0.1177	0.2	0.1269	0.1269	0.01
14	52.80	50.52	4.4	0.1380	0.1377	0.2	0.1513	0.1514	0.07

Table 6: Gluon fusion cross sections for scenario C.

Tables 7–9 display the cross section for associated $b\bar{b}\phi$ production in the three reference scenarios considered here. They list the total inclusive cross section as obtained in the 5FS, which can be calculated along with the $gg \to \phi$ cross section with SusHi; in addition, the 4FS result as obtained from the grids of the LHCHXSWG is displayed, see [31]. The third number, labeled "matched" in the table, corresponds to the combined result according to the Santander matching prescription:

$$\sigma_{\text{matched}} = \frac{\sigma^{\text{4FS}} + w\sigma^{\text{5FS}}}{1+w}\,, \tag{7}$$

where the weight function $w \equiv \ln(m_\phi/m_b) - 2$ is chosen such as to account for the excellent agreement of the two predictions at $m_\phi = 100\,\text{GeV}$, i.e., $w|_{m_\phi=100\text{GeV}} \approx 1$. We also recommend to follow Ref. [32] in determining the theoretical uncertainties.

$\sqrt{s}$	$\sigma(b\bar{b} \to h)$/pb			$\sigma(b\bar{b} \to H)$/pb $\cdot 10^4$			$\sigma(b\bar{b} \to A)$/pb $\cdot 10^3$		
/TeV	5FS	4FS	matched	5FS	4FS	matched	5FS	4FS	matched
7	0.239	0.221	0.231	1.45	1.18	1.37	1.49	1.19	1.39
8	0.310	0.293	0.302	2.07	1.69	1.95	2.15	1.74	2.02
13	0.743	0.727	0.736	6.56	5.58	6.25	7.08	5.96	6.74
14	0.842	0.822	0.833	7.70	6.68	7.38	8.36	7.13	7.98

Table 7: Associated $b\bar{b}\phi$ cross sections for scenario A. Note that the numbers for the heavy and the CP-odd Higgs are rescaled by a factor 10^4 and 10^3, respectively.

$\sqrt{s}$	$\sigma(b\bar{b} \to h)$/pb			$\sigma(b\bar{b} \to H)$/pb			$\sigma(b\bar{b} \to A)$/pb		
/TeV	5FS	4FS	matched	5FS	4FS	matched	5FS	4FS	matched
7	0.257	0.238	0.249	12.9	10.5	12.1	20.6	17.0	19.4
8	0.334	0.314	0.325	18.4	15.1	17.3	28.9	24.2	27.4
13	0.801	0.784	0.793	58.3	49.5	55.5	88.0	76.5	84.2
14	0.907	0.885	0.897	68.5	59.4	65.6	103	89.9	98.5

Table 8: Associated $b\bar{b}\phi$ cross sections for scenario B.

$\sqrt{s}$	$\sigma(b\bar{b} \to h)$/pb			$\sigma(b\bar{b} \to H)$/pb			$\sigma(b\bar{b} \to A)$/pb		
/TeV	5FS	4FS	matched	5FS	4FS	matched	5FS	4FS	matched
7	0.0513	0.0476	0.0497	0.135	0.104	0.126	0.0430	0.0318	0.0399
8	0.0667	0.0628	0.0650	0.200	0.156	0.187	0.0666	0.0500	0.0621
13	0.160	0.156	0.158	0.723	0.594	0.686	0.271	0.215	0.256
14	0.181	0.177	0.179	0.863	0.708	0.818	0.329	0.263	0.311

Table 9: Associated $b\bar{b}\phi$ cross sections for scenario C.

4.2 Branching ratios

Tables 10–12 show numerical results on the branching ratios and partial decay widths (in GeV) for the neutral Higgs bosons in scenarios A–C. In each table, the first two columns show the results obtained with `2HDMC-1.6.2`, the next two columns the same quantities computed with `HDECAY-6.00`, and the final column gives, for each decay, the ratio of calculated widths, $\Gamma_{\text{2HDMC}}/\Gamma_{\text{HDECAY}}$. Since the results from comparing `2HDMC` and `HDECAY` are qualitatively very similar for all three scenarios, we discuss Tables 10–12 together.

For decays calculated at leading order, the relative differences in the partial widths are at the level of 10^{-3} (or smaller) for all three neutral Higgs bosons. This includes the decays into lepton pairs, doube off-shell vector bosons, cascade Higgs decays, and mixed Higgs/vector boson final states, which are all in perfect agreement.

For the decays of the lightest Higgs boson, h, the largest relative difference is at the level of 2%, for the decay into $c\bar{c}$. Relative differences at the level of 1–2% are also observed for the $s\bar{s}$ final state, with a smaller deviation (0.8%) in the numerically most important result for $h \to b\bar{b}$. Similar numbers are found for the decays of the heavier Higgs bosons, H and A, into light quarks. It can be seen that these small differences are generic, and we have verified explicitly that they are due to small differences in the values of the running quark masses (which are evaluated at the scale of the Higgs mass for these decays).

For the phenomenologically important decay $h \to \gamma\gamma$, the level of agreement is better than 1%, whereas for $h \to gg$ the difference corresponds to around 1.3%. The same decays for the heavier Higgs boson show typically slightly larger deviations in the results, at the level of 2–3%. For these loop-induced decays, a residual difference of this magnitude is to be expected due to the different implementation of QCD corrections in the two codes (for details, see above). We have verified that this is indeed the source of the observed differences. One case where the full mass dependence in the QCD corrections becomes important is for the decays $H/A \to \gamma\gamma$ close to, or above, the $t\bar{t}$ threshold (cf. Scenarios A and C). Here, the full α_s corrections (as implemented in `HDECAY`) lead to a strong enhancement of this decay. However, since the corresponding branching ratios are very small, below 10^{-4}, this difference does not affect the total width (and not the branching ratios).

In all three reference scenarios, the calculated total widths of the neutral Higgs bosons agree at the sub-percent level between `2HDMC` and `HDECAY`, which demonstrates consistent results on the 2HDM branching ratios at a sufficient level of precision.

		2HDMC		HDECAY		
		BR	Γ (GeV)	BR	Γ (GeV)	$\Gamma_{\rm 2H}/\Gamma_{\rm HD}$
$h \to$	$b\bar{b}$	0.6812	3.790×10^{-3}	0.6827	3.820×10^{-3}	0.992
	$\tau^+\tau^-$	6.587×10^{-2}	3.664×10^{-4}	6.548×10^{-2}	3.664×10^{-4}	1.000
	$\mu^+\mu^-$	2.332×10^{-4}	1.297×10^{-6}	2.318×10^{-4}	1.297×10^{-6}	1.000
	$s\bar{s}$	2.484×10^{-4}	1.382×10^{-6}	2.503×10^{-4}	1.400×10^{-6}	0.987
	$c\bar{c}$	3.059×10^{-2}	1.701×10^{-4}	2.976×10^{-2}	1.665×10^{-4}	1.022
	gg	8.110×10^{-2}	4.511×10^{-4}	8.166×10^{-2}	4.569×10^{-4}	0.987
	$\gamma\gamma$	1.130×10^{-3}	6.284×10^{-6}	1.117×10^{-3}	6.250×10^{-6}	1.006
	$Z\gamma$	8.728×10^{-4}	4.855×10^{-6}	8.677×10^{-4}	4.855×10^{-6}	1.000
	W^+W^-	0.1233	6.859×10^{-4}	0.1226	6.860×10^{-4}	1.000
	ZZ	1.540×10^{-2}	8.569×10^{-5}	1.531×10^{-2}	8.566×10^{-5}	1.000
Total width			$\mathbf{5.563 \times 10^{-3}}$		$\mathbf{5.595 \times 10^{-3}}$	**0.994**
$H \to$	$b\bar{b}$	8.492×10^{-5}	1.536×10^{-4}	8.526×10^{-5}	1.542×10^{-4}	0.996
	$\tau^+\tau^-$	9.667×10^{-6}	1.748×10^{-5}	9.667×10^{-6}	1.748×10^{-5}	1.000
	$\mu^+\mu^-$	3.419×10^{-8}	6.182×10^{-8}	3.419×10^{-8}	6.183×10^{-8}	1.000
	$s\bar{s}$	3.070×10^{-8}	5.552×10^{-8}	3.115×10^{-7}	5.636×10^{-8}	0.985
	$c\bar{c}$	3.787×10^{-6}	6.848×10^{-6}	3.706×10^{-6}	6.706×10^{-6}	1.021
	$t\bar{t}$	5.976×10^{-6}	1.081×10^{-5}	5.986×10^{-6}	1.082×10^{-5}	0.998
	gg	8.382×10^{-5}	1.516×10^{-4}	8.669×10^{-5}	1.568×10^{-4}	0.967
	$\gamma\gamma$	1.642×10^{-5}	2.969×10^{-5}	1.653×10^{-5}	2.989×10^{-5}	0.993
	$Z\gamma$	5.300×10^{-5}	9.584×10^{-5}	5.300×10^{-5}	9.584×10^{-5}	1.000
	W^+W^-	0.5872	1.062	0.5872	1.062	1.000
	ZZ	0.2606	0.4713	0.2606	0.4712	1.000
	hh	0.1493	0.2699	0.1493	0.2700	1.000
	$W^\pm H^\mp$	2.658×10^{-3}	4.806×10^{-3}	2.663×10^{-3}	4.815×10^{-3}	0.998
Total width			**1.808**		**1.808**	**1.000**
$A \to$	$b\bar{b}$	1.568×10^{-3}	2.564×10^{-3}	1.573×10^{-3}	2.572×10^{-3}	0.997
	$\tau^+\tau^-$	1.859×10^{-4}	3.039×10^{-4}	1.858×10^{-4}	3.038×10^{-4}	1.000
	$\mu^+\mu^-$	6.573×10^{-7}	1.075×10^{-6}	6.571×10^{-7}	1.075×10^{-6}	1.000
	$s\bar{s}$	5.385×10^{-7}	8.804×10^{-7}	5.466×10^{-7}	8.939×10^{-7}	0.985
	$c\bar{c}$	7.219×10^{-5}	1.180×10^{-4}	7.067×10^{-5}	1.156×10^{-4}	1.021
	$t\bar{t}$	1.395×10^{-2}	2.280×10^{-2}	1.399×10^{-2}	2.288×10^{-2}	0.997
	gg	8.874×10^{-3}	1.451×10^{-2}	9.060×10^{-3}	1.482×10^{-2}	0.979
	$\gamma\gamma$	2.380×10^{-5}	3.891×10^{-5}	3.155×10^{-5}	5.159×10^{-5}	0.754
	$Z\gamma$	5.725×10^{-6}	9.360×10^{-6}	5.724×10^{-6}	9.361×10^{-6}	1.000
	Zh	0.5747	0.9396	0.5746	0.9397	1.000
	ZH	2.221×10^{-6}	9.852×10^{-6}	6.029×10^{-6}	9.859×10^{-6}	0.999
	$W^\pm H^\mp$	0.4006	0.6550	0.4005	0.6550	1.000
Total width			**1.635**		**1.635**	**1.000**

Table 10: Numerical comparison between neutral Higgs branching ratios and decay widths calculated with 2HDMC and HDECAY for reference scenario A.

		2HDMC		HDECAY		
		BR	Γ (GeV)	BR	Γ (GeV)	$\Gamma_{\rm 2H}/\Gamma_{\rm HD}$
$h \to$	$b\bar{b}$	0.6794	4.018×10^{-3}	0.6809	4.051×10^{-3}	0.992
	$\tau^+\tau^-$	6.672×10^{-2}	3.946×10^{-4}	6.633×10^{-2}	3.947×10^{-4}	1.000
	$\mu^+\mu^-$	2.362×10^{-4}	1.397×10^{-6}	2.348×10^{-4}	1.397×10^{-6}	1.000
	$s\bar{s}$	2.384×10^{-4}	1.410×10^{-6}	2.402×10^{-6}	1.429×10^{-6}	0.987
	$c\bar{c}$	2.031×10^{-2}	1.201×10^{-4}	1.975×10^{-2}	1.175×10^{-4}	1.022
	gg	7.043×10^{-2}	4.166×10^{-4}	7.089×10^{-2}	4.218×10^{-4}	0.988
	$\gamma\gamma$	1.391×10^{-3}	8.229×10^{-6}	1.375×10^{-3}	8.181×10^{-6}	1.006
	$Z\gamma$	1.013×10^{-3}	5.994×10^{-6}	1.003×10^{-3}	5.968×10^{-6}	1.004
	W^+W^-	0.1425	8.427×10^{-4}	0.1416	8.425×10^{-4}	1.000
	ZZ	1.780×10^{-2}	1.053×10^{-4}	1.769×10^{-2}	1.053×10^{-4}	1.000
Total width			$\mathbf{5.915 \times 10^{-3}}$		$\mathbf{5.950 \times 10^{-3}}$	**0.994**
$H \to$	$b\bar{b}$	0.8947	13.52	0.8950	13.58	0.996
	$\tau^+\tau^-$	0.1028	1.553	0.1024	1.553	1.000
	$\mu^+\mu^-$	3.635×10^{-4}	5.494×10^{-3}	3.621×10^{-4}	5.494×10^{-3}	1.000
	$s\bar{s}$	3.172×10^{-4}	4.795×10^{-3}	3.208×10^{-4}	4.867×10^{-3}	0.985
	$c\bar{c}$	9.829×10^{-9}	1.486×10^{-7}	9.590×10^{-9}	1.455×10^{-7}	1.021
	gg	4.477×10^{-4}	6.676×10^{-3}	4.604×10^{-4}	6.985×10^{-3}	0.969
	$\gamma\gamma$	1.044×10^{-7}	1.578×10^{-6}	1.075×10^{-7}	1.631×10^{-6}	0.968
	$Z\gamma$	1.034×10^{-7}	1.562×10^{-6}	1.027×10^{-7}	1.558×10^{-6}	1.003
	W^+W^-	7.474×10^{-4}	1.130×10^{-2}	7.447×10^{-4}	1.130×10^{-2}	1.000
	ZZ	3.317×10^{-4}	5.014×10^{-3}	3.305×10^{-4}	5.014×10^{-3}	1.000
	hh	3.493×10^{-4}	5.280×10^{-3}	3.481×10^{-7}	5.281×10^{-3}	1.000
	ZA	7.891×10^{-7}	1.193×10^{-5}	7.869×10^{-7}	1.194×10^{-5}	0.999
Total width			**15.12**		**15.17**	**0.996**
$A \to$	$b\bar{b}$	0.8975	12.42	0.8979	12.47	0.996
	$\tau^+\tau^-$	0.1010	1.399	0.1007	1.399	1.000
	$\mu^+\mu^-$	3.573×10^{-4}	4.946×10^{-3}	3.561×10^{-4}	4.946×10^{-3}	1.000
	$s\bar{s}$	3.179×10^{-4}	4.401×10^{-3}	3.217×10^{-4}	4.468×10^{-3}	0.985
	$c\bar{c}$	6.514×10^{-9}	9.018×10^{-8}	6.358×10^{-9}	8.830×10^{-8}	1.021
	gg	5.648×10^{-4}	7.818×10^{-3}	5.741×10^{-4}	7.973×10^{-3}	0.981
	$\gamma\gamma$	1.126×10^{-7}	1.559×10^{-6}	1.089×10^{-7}	1.512×10^{-6}	1.031
	$Z\gamma$	5.261×10^{-8}	7.283×10^{-7}	5.238×10^{-8}	7.275×10^{-7}	1.001
	Zh	1.957×10^{-4}	2.710×10^{-3}	1.951×10^{-4}	2.710×10^{-3}	1.000
Total width			**13.84**		**13.89**	**0.997**

Table 11: Numerical comparison between neutral Higgs branching ratios and decay widths calculated with 2HDMC and HDECAY for reference scenario B.

		2HDMC		HDECAY		
		BR	Γ (GeV)	BR	Γ (GeV)	$\Gamma_{\rm 2H}/\Gamma_{\rm HD}$
$h \to$	$b\bar{b}$	0.3536	8.207×10^{-4}	0.3551	8.272×10^{-4}	0.992
	$\tau^+\tau^-$	3.395×10^{-2}	7.880×10^{-5}	3.383×10^{-2}	7.881×10^{-5}	1.000
	$\mu^+\mu^-$	1.202×10^{-4}	2.790×10^{-7}	1.198×10^{-4}	2.791×10^{-7}	1.000
	$s\bar{s}$	1.311×10^{-4}	3.042×10^{-7}	1.323×10^{-4}	3.028×10^{-7}	0.987
	$c\bar{c}$	5.211×10^{-2}	1.210×10^{-4}	5.082×10^{-2}	1.184×10^{-4}	1.022
	gg	0.1453	3.374×10^{-4}	0.1467	3.417×10^{-4}	0.987
	$\gamma\gamma$	3.791×10^{-3}	8.799×10^{-6}	3.761×10^{-3}	8.761×10^{-6}	1.004
	$Z\gamma$	2.627×10^{-3}	6.098×10^{-6}	2.681×10^{-3}	6.099×10^{-6}	1.000
	W^+W^-	0.3630	8.427×10^{-4}	0.3617	8.426×10^{-4}	1.000
	ZZ	4.535×10^{-2}	1.053×10^{-4}	4.519×10^{-2}	1.053×10^{-4}	1.000
Total width			$\mathbf{2.321 \times 10^{-3}}$		$\mathbf{2.329 \times 10^{-3}}$	**0.996**
$H \to$	$b\bar{b}$	0.7671	0.6903	0.7675	0.6926	0.997
	$\tau^+\tau^-$	9.273×10^{-2}	8.345×10^{-2}	9.247×10^{-2}	8.344×10^{-2}	1.000
	$\mu^+\mu^-$	3.279×10^{-4}	2.951×10^{-4}	3.270×10^{-4}	2.951×10^{-4}	1.000
	$s\bar{s}$	2.717×10^{-4}	2.445×10^{-4}	2.751×10^{-4}	2.483×10^{-4}	0.985
	$c\bar{c}$	1.044×10^{-6}	9.392×10^{-7}	1.019×10^{-6}	9.195×10^{-7}	1.021
	$t\bar{t}$	1.416×10^{-2}	1.274×10^{-2}	1.436×10^{-2}	1.296×10^{-2}	0.983
	gg	5.203×10^{-4}	4.682×10^{-4}	5.358×10^{-4}	4.835×10^{-4}	0.968
	$\gamma\gamma$	1.188×10^{-6}	1.069×10^{-6}	1.319×10^{-6}	1.190×10^{-6}	0.898
	$Z\gamma$	1.764×10^{-6}	1.588×10^{-6}	1.759×10^{-6}	1.587×10^{-6}	1.000
	W^+W^-	3.586×10^{-2}	3.227×10^{-2}	3.576×10^{-2}	3.227×10^{-2}	1.000
	ZZ	1.672×10^{-2}	1.504×10^{-2}	1.667×10^{-2}	1.504×10^{-2}	1.000
	hh	7.229×10^{-2}	6.505×10^{-2}	7.209×10^{-2}	6.505×10^{-2}	1.000
Total width			**0.8999**		**0.9024**	**0.997**
$A \to$	$b\bar{b}$	0.6117	0.8253	0.6138	0.8274	0.997
	$\tau^+\tau^-$	7.679×10^{-2}	0.1036	7.684×10^{-2}	0.1036	1.000
	$\mu^+\mu^-$	2.716×10^{-4}	3.663×10^{-4}	2.717×10^{-4}	3.663×10^{-3}	1.000
	$s\bar{s}$	2.166×10^{-4}	2.923×10^{-4}	2.200×10^{-4}	2.966×10^{-4}	0.986
	$c\bar{c}$	2.774×10^{-6}	3.742×10^{-6}	2.717×10^{-6}	3.663×10^{-6}	1.022
	$t\bar{t}$	0.1690	0.2279	0.1668	0.2248	1.014
	gg	8.384×10^{-4}	1.131×10^{-3}	8.560×10^{-4}	1.154×10^{-3}	0.980
	$\gamma\gamma$	1.761×10^{-6}	2.376×10^{-6}	1.860×10^{-6}	2.507×10^{-6}	0.948
	$Z\gamma$	4.851×10^{-7}	6.545×10^{-7}	4.854×10^{-7}	6.543×10^{-7}	1.000
	Zh	4.426×10^{-2}	5.971×10^{-2}	4.428×10^{-2}	5.969×10^{-2}	1.000
	ZH	9.694×10^{-2}	0.1308	9.699×10^{-2}	0.1307	1.000
Total width			**1.349**		**1.348**	**1.001**

Table 12: Numerical comparison between neutral Higgs branching ratios and decay widths calculated with 2HDMC and HDECAY for reference scenario C.

5 Conclusions

We have described the current status of theoretical predictions for the gluon fusion and associated $b\bar{b}\phi$ Higgs production processes as well as the Higgs branching ratios within the 2HDM. The theoretical tools recommended for their evaluation are `HIGLU` and `SusHi` for the total inclusive cross sections, and `2HDMC` and `HDECAY` for the decay rates and branching ratios. These programs are publically available from the following URLs:

```
SusHi:   http://sushi.hepforge.org/
2HDMC:   http://2hdmc.hepforge.org/
HIGLU:   http://people.web.psi.ch/spira/higlu/
HDECAY:  http://people.web.psi.ch/spira/hdecay/
```

Please always use the latest versions of these programs; the results presented in this note have been obtained with `2HDMC-1.6.2`, `HDECAY-6.00`, `HIGLU-4.00`, and `SusHi-1.1.1`. Earlier versions of these programs must not be used to obtain viable 2HDM results.

Currently, `SusHi` and `2HDMC` can be linked to each other, and run with a single input file. In addition a similar approach has been adopted for `HIGLU` and `HDECAY` which are linked but work with two input files, i.e. the usual input file of `HDECAY` and an additional one for `HIGLU` that specifies properties of the production cross sections to be calculated beyond the input values of `HDECAY`.

Acknowledgements

We thank the members of the Heavy Higgs Group of the LHC Higgs cross section working group for useful discussions. In particular we are grateful to Nikolaos Rompotis for useful comments and suggestions. M.M. thanks Rui Santos for helpful discussions. R.H. is supported by BMBF (grant no. 05H12PXE) and DFG (grant no. HA 2990/6-1). M.M. is supported by the DFG SFB/TR9 "Computational Particle Physics". J.R. is supported in part by the Swedish Research Council under contracts 621-2011-5333 and 621-2013-4287. O.S. is supported by the Swedish Research Council (VR) through the Oskar Klein Centre.

References

[1] G. C. Branco, P. M. Ferreira, L. Lavoura, M. N. Rebelo, M. Sher and J. P. Silva, Phys. Rept. **516**, 1 (2012) [arXiv:1106.0034 [hep-ph]].

[2] R. V. Harlander and W. B. Kilgore, Phys. Rev. Lett. **88** (2002) 201801 [hep-ph/0201206].

[3] C. Anastasiou and K. Melnikov, Nucl. Phys. B **646** (2002) 220 [hep-ph/0207004].

[4] V. Ravindran, J. Smith and W. L. van Neerven, Nucl. Phys. B **665** (2003) 325 [hep-ph/0302135].

[5] D. Graudenz, M. Spira and P. M. Zerwas, Phys. Rev. Lett. **70** (1993) 1372.

[6] M. Spira, A. Djouadi, D. Graudenz and P. M. Zerwas, Phys. Lett. B **318** (1993) 347.

[7] M. Spira, A. Djouadi, D. Graudenz and P. M. Zerwas, Nucl. Phys. B **453** (1995) 17 [hep-ph/9504378].

[8] S. Marzani, R. D. Ball, V. Del Duca, S. Forte and A. Vicini, Nucl. Phys. Proc. Suppl. **186** (2009) 98 [arXiv:0809.4934 [hep-ph]].

[9] R. V. Harlander, H. Mantler, S. Marzani and K. J. Ozeren, Eur. Phys. J. C **66** (2010) 359 [arXiv:0912.2104 [hep-ph]].

[10] R. V. Harlander and K. J. Ozeren, JHEP **0911** (2009) 088 [arXiv:0909.3420 [hep-ph]].

[11] A. Pak, M. Rogal and M. Steinhauser, JHEP **1002** (2010) 025 [arXiv:0911.4662 [hep-ph]].

[12] A. Pak, M. Rogal and M. Steinhauser, JHEP **1109** (2011) 088 [arXiv:1107.3391 [hep-ph]].

[13] R. V. Harlander, S. Liebler and H. Mantler, Comp. Phys. Commun. **184** (2013) 1605 [arXiv:1212.3249 [hep-ph]].

[14] M. Spira, hep-ph/9510347 and Nucl. Instrum. Meth. A **389** (1997) 357.

[15] S. Catani, D. de Florian, M. Grazzini and P. Nason, JHEP **0307** (2003) 028 [hep-ph/0306211].

[16] V. Ravindran, Nucl. Phys. B **746** (2006) 58 and Nucl. Phys. B **752** (2006) 173.

[17] C. Anastasiou, R. Boughezal and F. Petriello, JHEP **0904** (2009) 003 [arXiv:0811.3458 [hep-ph]].

[18] S. Moch and A. Vogt, Phys. Lett. B **631** (2005) 48 [hep-ph/0508265].

[19] R. D. Ball, M. Bonvini, S. Forte, S. Marzani and G. Ridolfi, Nucl. Phys. B **874** (2013) 746 [arXiv:1303.3590 [hep-ph]].

[20] A. Djouadi and P. Gambino, Phys. Rev. Lett. **73** (1994) 2528 [hep-ph/9406432].

[21] S. Actis, G. Passarino, C. Sturm and S. Uccirati, Phys. Lett. B **670** (2008) 12 [arXiv:0809.1301 [hep-ph]].

[22] G. Degrassi and F. Maltoni, Phys. Lett. B **600** (2004) 255 [hep-ph/0407249].

[23] U. Aglietti, R. Bonciani, G. Degrassi and A. Vicini, Phys. Lett. B **595** (2004) 432 [hep-ph/0404071].

[24] D. A. Dicus and S. Willenbrock, Phys. Rev. D **39** (1989) 751.

[25] J. M. Campbell, R. K. Ellis, F. Maltoni and S. Willenbrock, Phys. Rev. D **67** (2003) 095002 [hep-ph/0204093].

[26] D. Dicus, T. Stelzer, Z. Sullivan and S. Willenbrock, Phys. Rev. D **59** (1999) 094016 [hep-ph/9811492].

[27] F. Maltoni, Z. Sullivan and S. Willenbrock, Phys. Rev. D **67** (2003) 093005 [hep-ph/0301033].

[28] S. Dittmaier, M. Krämer and M. Spira, Phys. Rev. D **70** (2004) 074010 [hep-ph/0309204].

[29] S. Dawson, C. B. Jackson, L. Reina and D. Wackeroth, Phys. Rev. D **69** (2004) 074027 [hep-ph/0311067].

[30] R. V. Harlander and W. B. Kilgore, Phys. Rev. D **68** (2003) 013001 [hep-ph/0304035].

[31] The files `4f_pseudoscalar_7.root`, `4f_pseudoscalar_8.root`, `4f_scalar_7.root` and `4f_scalar_8.root` containing the 4FS MSSM numbers can be found at `https://svnweb.cern.ch/cern/wsvn/lhchiggsxs/repository/MSSM/Neutral Higgs/machinery_with_SusHI/root_files/?#a6f5d38d4636ed77fc65dc5f03a8bdcb5`; `https://twiki.cern.ch/twiki/bin/view/LHCPhysics/MSSMNeutral`.

[32] R. Harlander, M. Krämer and M. Schumacher, arXiv:1112.3478 [hep-ph].

[33] S. D. Thomas, `https://indico.cern.ch/getFile.py/access?contribId=4&resId=1 &materialId=slides&confId=270897`

[34] R. K. Ellis, I. Hinchliffe, M. Soldate and J. J. van der Bij, Nucl. Phys. B **297** (1988) 221; U. Baur and E.W.N. Glover, Nucl. Phys. B **339** (1990) 38; O. Brein and W. Hollik, Phys. Rev. D **68** (2003) 095006; U. Langenegger, M. Spira, A. Starodumov and P. Trüb, JHEP **0606** (2006) 035.

[35] C. R. Schmidt, Phys. Lett. B **413** (1997) 391; D. de Florian, M. Grazzini and Z. Kunszt, Phys. Rev. Lett. **82** (1999) 5209; V. Ravindran, J. Smith and W. L. Van Neerven, Nucl. Phys. B **634** (2002) 247; C. J. Glosser and C. R. Schmidt, JHEP **0212** (2002) 016; C. Anastasiou, K. Melnikov and F. Petriello, Phys. Rev. Lett. **93** (2004) 262002 and Nucl. Phys. B **724** (2005) 197.

[36] R. Boughezal, F. Caola, K. Melnikov, F. Petriello and M. Schulze, JHEP **1306** (2013) 072.

[37] R.V. Harlander, T. Neumann, K.J. Ozeren and M. Wiesemann, JHEP **1208** (2012) 139.

[38] S. Catani, E. D'Emilio and L. Trentadue, Phys. Lett. B **211** (1988) 335; I. Hinchliffe and S.F. Novaes, Phys. Rev. D **38** (1988) 3475; R. P. Kauffman, Phys. Rev. D **44** (1991) 1415 and Phys. Rev. D **45** (1992) 1512; C. Balazs and C.P. Yuan, Phys. Lett. B **478** (2000) 192; E. L. Berger and J.W. Qiu, Phys. Rev. D **67** (2003) 034026; A. Kulesza and W. J. Stirling, JHEP **0312** (2003) 056; A. Kulesza, G. Sterman and W. Vogelsang, Phys. Rev. D **69** (2004) 014012; A. Gawron and J. Kwiecinski, Phys. Rev. D **70** (2004) 014003; G. Watt, A. D. Martin and M. G. Ryskin, Phys. Rev. D **70** (2004) 014012 [Erratum-ibid. D **70** (2004) 079902]; A. V. Lipatov and N. P. Zotov, Eur. Phys. J. C **44** (2005) 559; D. de Florian and M. Grazzini, Phys. Rev. Lett. **85** (2000) 4678; Nucl. Phys. B **616** (2001) 247; S. Catani, D. de Florian and M. Grazzini, Nucl. Phys. B **596** (2001) 299; G. Bozzi, S. Catani, D. de Florian and M. Grazzini, Phys. Lett. B **564** (2003) 65; G. Bozzi, S. Catani, D. de Florian and M. Grazzini, Nucl. Phys. B **737** (2006) 73 and Nucl. Phys. B **791** (2008) 1; D. de Florian, G. Ferrera, M. Grazzini and D. Tommasini, JHEP **1111** (2011) 064.

[39] J. Alwall, Q. Li and F. Maltoni, Phys. Rev. D **85** (2012) 014031 [arXiv:1110.1728 [hep-ph]].

[40] E. Bagnaschi, G. Degrassi, P. Slavich and A. Vicini, JHEP **1202** (2012) 088 [arXiv:1111.2854 [hep-ph]].

[41] H. Mantler and M. Wiesemann, Eur. Phys. J. C **73** (2013) 2467 [arXiv:1210.8263 [hep-ph]].

[42] `http://theory.fi.infn.it/grazzini/codes.html`

[43] M. Grazzini and H. Sargsyan, JHEP **1309** (2013) 129 [arXiv:1306.4581 [hep-ph]].

[44] A. Banfi, P. F. Monni and G. Zanderighi, arXiv:1308.4634 [hep-ph].

[45] S. Frixione and B. R. Webber, JHEP **0206** (2002) 029 [hep-ph/0204244].

[46] http://www.hep.phy.cam.ac.uk/theory/webber/MCatNLO

[47] J. M. Campbell, S. Dawson, S. Dittmaier, C. Jackson, M. Krämer, F. Maltoni, L. Reina, M. Spira, D. Wackeroth and S. Willenbrock, hep-ph/0405302.

[48] R. V. Harlander, K. J. Ozeren and M. Wiesemann, Phys. Lett. B **693** (2010) 269 [arXiv:1007.5411 [hep-ph]].

[49] http://mcfm.fnal.gov/

[50] R. Harlander and M. Wiesemann, JHEP **1204** (2012) 066 [arXiv:1111.2182 [hep-ph]].

[51] S. Bühler, F. Herzog, A. Lazopoulos and R. Müller, JHEP **1207** (2012) 115 [arXiv:1204.4415 [hep-ph]].

[52] A. Belyaev, P. M. Nadolsky and C. -P. Yuan, JHEP **0604** (2006) 004 [hep-ph/0509100].

[53] http://amcatnlo.web.cern.ch/amcatnlo/

[54] D. Eriksson, J. Rathsman and O. Stål, Comput. Phys. Commun. **181**, 189 (2010) [arXiv:0902.0851 [hep-ph]]; D. Eriksson, J. Rathsman and O. Stål, Comput. Phys. Commun. **181**, 833 (2010).

[55] A. Djouadi, J. Kalinowski and M. Spira, Comput. Phys. Commun. **108**, 56 (1998) [hep-ph/9704448]; A. Djouadi, M. M. Mühlleitner and M. Spira, Acta Phys. Polon. B **38** (2007) 635 [hep-ph/0609292].

[56] M. Spira, Fortsch. Phys. **46** (1998) 203 [hep-ph/9705337]; A. Djouadi, Phys. Rept. **459** (2008) 1 [hep-ph/0503173].

[57] S. Davidson and H. E. Haber, Phys. Rev. D **72**, 035004 (2005) [Erratum-ibid. D **72**, 099902 (2005)] [hep-ph/0504050].

[58] V. D. Barger, J. L. Hewett and R. J. N. Phillips, Phys. Rev. D **41**, 3421 (1990).

[59] P. Bechtle, O. Brein, S. Heinemeyer, G. Weiglein and K. E. Williams, Comput. Phys. Commun. **181**, 138 (2010) [arXiv:0811.4169 [hep-ph]]; P. Bechtle, O. Brein, S. Heinemeyer, G. Weiglein and K. E. Williams, Comput. Phys. Commun. **182**, 2605 (2011) [arXiv:1102.1898 [hep-ph]]; P. Bechtle, O. Brein, S. Heinemeyer, O. Stål, T. Stefaniak, G. Weiglein and K. E. Williams, arXiv:1311.0055 [hep-ph].

[60] E. Braaten and J. P. Leveille, Phys. Rev. D **22** (1980) 715; N. Sakai, Phys. Rev. D **22** (1980) 2220; T. Inami and T. Kubota, Nucl. Phys. B **179** (1981) 171; M. Drees and K.–I. Hikasa, Phys. Rev. D **41** (1990) 1547; M. Drees and K.–I. Hikasa, Phys. Lett. B **240** (1990) 455 [Erratum-ibid. B **262** (1991) 497].

[61] S. G. Gorishnii, A. L. Kataev, S. A. Larin and L. R. Surguladze, Mod. Phys. Lett. A **5** (1990) 2703; S. G. Gorishnii, A. L. Kataev, S. A. Larin and L. R. Surguladze, Phys.Rev. D **43** (1991) 1633; A. L. Kataev and V. T. Kim, Mod. Phys. Lett. A **9** (1994) 1309; S. G. Gorishnii, A. L. Kataev and S. A. Larin, Sov. J. Nucl. Phys. **40** (1984) 329 [Yad. Fiz. 40 (1984) 517]; L. R. Surguladze, Phys. Lett. B **341** (1994) 60 [hep-ph/9405325]; S. A. Larin, T. van Ritbergen and J. A. M. Vermaseren, Phys. Lett. B **362** (1995) 134 [hep-ph/9506465]; K. G. Chetyrkin and A. Kwiatkowski, Nucl. Phys. B **461** (1996) 3 [hep-ph/9505358].

[62] K. G. Chetyrkin, Phys. Lett. B **390** (1997) 309 [hep-ph/9608318].

[63] P. A. Baikov, K. G. Chetyrkin and J. H. Kühn, Phys. Rev. Lett. **96** (2006) 012003 [hep-ph/0511063].

[64] A. Mendez and A. Pomarol, Phys. Lett. B **252** (1990) 461; C.–S. Li and R. J. Oakes, Phys. Rev. D **43** (1991) 855; A. Djouadi and P. Gambino, Phys. Rev. D **51** (1995) 218 [Erratum-ibid. D **53** (1996) 4111] [hep-ph/9406431].

[65] A. Djouadi, J. Kalinowski and P. M. Zerwas, Z. Phys. C **70** (1996) 437; S. Moretti and W. J. Stirling, Phys. Lett. B **347** (1995) 291 and (E) B **366** (1996) 451.

[66] T. Inami, T. Kubota and Y. Okada, Z. Phys. C **18** (1983) 69; A. Djouadi, M. Spira and P. M. Zerwas, Phys. Lett. B **264** (1991) 440; K. G. Chetyrkin, B. A. Kniehl and M. Steinhauser, Phys. Rev. Lett. **79** (1997) 353 [hep-ph/9705240]; K. G. Chetyrkin, B. A. Kniehl, M. Steinhauser and W. A. Bardeen, Nucl. Phys. B **535**, 3 (1998) [hep-ph/9807241].

[67] K. G. Chetyrkin, B. A. Kniehl and M. Steinhauser, Nucl. Phys. B **510** (1998) 61 [hep-ph/9708255].

[68] P. A. Baikov and K. G. Chetyrkin, Phys. Rev. Lett. **97** (2006) 061803 [hep-ph/0604194].

[69] A. Djouadi, M. Spira and P. M. Zerwas, Phys. Lett. B **311** (1993) 255;

[70] H.–Q. Zheng and D.–D. Wu, Phys. Rev. D **42** (1990) 3760; A. Djouadi, M. Spira, J. J. van der Bij and P. M. Zerwas, Phys. Lett. B **257** (1991) 187; S. Dawson and R. P. Kauffman, Phys. Rev. D **47** (1993) 1264; A. Djouadi, M. Spira and P. M. Zerwas, Phys. Lett. B **311** (1993) 255 [hep-ph/9305335]; K. Melnikov and O. I. Yakovlev, Phys. Lett. B **312** (1993) 179 [hep-ph/9302281]; M. Inoue, R. Najima, T. Oka and J. Saito, Mod. Phys. Lett. A **9** (1994) 1189; J. Fleischer, O. V. Tarasov and V. O. Tarasov, Phys. Lett. B **584** (2004) 294 [hep-ph/0401090].

[71] A. Djouadi, M. Spira, J. J. van der Bij and P. M. Zerwas, Phys. Lett. B **257** (1991) 187; K. Melnikov and O. Yakovlev, Phys. Lett. B **312** (1993) 179; M. Inoue, R. Najima, T. Oka and J. Saito, Mod. Phys. Lett. A **9** (1994) 1189.

[72] M. Spira, A. Djouadi and P. M. Zerwas, Phys. Lett. B **276** (1992) 350.

[73] R.N. Cahn, Rept. Prog. Phys. **52** (1989) 389.

[74] S. Dittmaier *et al.* [LHC Higgs Cross Section Working Group Collaboration], arXiv:1101.0593 [hep-ph].

[75] PDF4LHC steering committee, `http://www.hep.ucl.ac.uk/pdf4lhc/`.

A SM parameters

For the numerical comparisons presented in this note, the following set of SM input parameters has been adopted. The numbers are given in the input style of HDECAY, but the same parameter values were used with 2HDMC.

```
ALS(MZ)  = 0.119D0
MSBAR(2) = 0.100D0
MC       = 1.42D0
MB       = 4.75D0
MT       = 172.5D0
MTAU     = 1.77684D0
MMUON    = 0.105658367D0
1/ALPHA  = 137.0359997D0
GF       = 1.16637D-5
GAMW     = 2.08856D0
GAMZ     = 2.49581D0
MZ       = 91.15349D0
MW       = 80.36951D0
VTB      = 0.9991D0
VTS      = 0.0404D0
VTD      = 0.00867D0
VCB      = 0.0412D0
VCS      = 0.97344D0
VCD      = 0.22520D0
VUB      = 0.00351D0
VUS      = 0.22534D0
VUD      = 0.97427D0
```

In both codes, 2HDMC and HDECAY, three-loop running of the strong coupling has been used. Matching between the quark flavor thresholds was performed at the pole masses, taking into account threshold corrections to $\mathcal{O}(\alpha_s^2)$. The running quark masses have been computed at one loop in the $\overline{\rm MS}$ scheme from the input pole masses given above, and running was then performed at three loops with matching at the pole masses. Threshold corrections have not been included for the running quark masses. Note in addition that the W and Z masses correspond to the pole masses in the complex-mass scheme, and that the top and bottom quark masses correspond to the standard choices of the SM input parameters of the LHC Higgs Cross Sections Working Group [74].